

Journal of Receptors and Signal Transduction

ISSN: (Print) (Online) Journal homepage: https://www.tandfonline.com/loi/irst20

Clostridium botulinum neurotoxin A induces apoptosis and mitochondrial oxidative stress via activation of TRPM2 channel signaling pathway in neuroblastoma and glioblastoma tumor cells

Orhan Akpınar , Ahmet Özşimşek , Mustafa Güzel & Mustafa Nazıroğlu

To cite this article: Orhan Akpınar , Ahmet Özşimşek , Mustafa Güzel & Mustafa Nazıroğlu (2020): *Clostridium botulinum* neurotoxin A induces apoptosis and mitochondrial oxidative stress via activation of TRPM2 channel signaling pathway in neuroblastoma and glioblastoma tumor cells, Journal of Receptors and Signal Transduction, DOI: 10.1080/10799893.2020.1781174

To link to this article: https://doi.org/10.1080/10799893.2020.1781174

Published online: 09 Jul 2020.

Submit your article to this journal

View related articles

View Crossmark data

Full Terms & Conditions of access and use can be found at
https://www.tandfonline.com/action/journalInformation?journalCode=irst20

JOURNAL OF RECEPTORS AND SIGNAL TRANSDUCTION
https://doi.org/10.1080/10799893.2020.1781174

Taylor & Francis
Taylor & Francis Group

ORIGINAL ARTICLE

Check for updates

Clostridium botulinum neurotoxin A induces apoptosis and mitochondrial oxidative stress via activation of TRPM2 channel signaling pathway in neuroblastoma and glioblastoma tumor cells

Orhan Akpınar[a,b], Ahmet Özşimşek[c], Mustafa Güzel[d] and Mustafa Nazıroğlu[e,f]

[a]Unit of Medical Microbiology, Department of Oral and Maxillofacial Surgery, Faculty of Dentistry, Suleyman Demirel University, Isparta, Turkey; [b]Departmant of Medical Microbiology, Health Sciences Institute, Suleyman Demirel University, Isparta, Turkey; [c]Department of Neurology, Faculty of Medicine, Alanya Alaaddin Keykubat University, Antalya, Turkey; [d]Department of Medical Microbiology, Private Maltepe Medical Center, Istanbul, Turkey; [e]Neuroscience Research Center, Suleyman Demirel University, Isparta, Turkey; [f]Drug Discovery Unit, BSN Health, Analyses, Innovation, Consultancy, Organization, Agriculture, Industry and Trade Limited Company, Göller Bölgesi Teknokenti, Isparta, Turkey

ABSTRACT

Background: The *Clostridium botulinum* neurotoxin A (BTX) is a polypeptide produced by the bacterium *Clostridium botulinum*. In addition to the therapeutic actions of BTX against pain and neuromuscular disorders, it is acted as anticancerogenic effect through excessive mitochondria reactive oxygen species (ROS) production, apoptosis, and caspase activations. The TRPM2 cation channel is activated by ROS and ADP-ribose and it is inhibited by 2-aminoethyl diphenylborinate (2-APB) and N-(p-amylcinnamoyl) anthranilic acid (ACA). The aim of this study was an investigation of involvement BTX-induced TRPM2 activation on the mitochondria ROS production and apoptosis levels in the DBTRG glioblastoma and SH-SY5Y neuroblastoma tumor cells.

Material and methods: The DBTRG and SH-SY5Y cells were divided into four groups as control, BTX (5 IU for 24 h), BTX + ACA (25 μM for 30 min), and BTX + 2-APB (100 μM for 30 min).

Results: BTX treatment increased mitochondrial membrane depolarization (JC-1), mitochondrial (MitROS), and cytosolic (DHR123 and DCFH-DA) ROS levels, neuronal death (propidium iodide/Hoechst) rate, caspase −3, and −9 levels in the BTX group, although their levels were diminished in the BTX + ACA and BTX + 2-APB groups. The ACA and 2-APB treatments also decreased BTX-induced increase of TRPM2 cytosolic free Ca^{2+} concentration in the glioblastoma and neuroblastoma cell death.

Conclusions: BTX caused neuroblastoma and glioblastoma tumor cell death by activating the mitochondria ROS production *via* stimulating TRPM2 signaling pathways. BTX may serve as a potential therapeutic target *via* activation of TRPM2 for treating glioblastoma and neuroblastoma cells.

Abbreviations: 2-APB: 2-aminoethyl diphenylborinate; ACA: N-(p-amylcinnamoyl) anthranilic acid; ADPR: ADP-ribose; BTX: clostridium botulinum neurotoxin A; DCF: 2′,7′-dichlorofluorescein; DCFH-DA: 2′,7′-dichlorodihydrofluorescin diacetate; DMEM: Dulbecco's Modified Eagle's Medium; H_2O_2: hydrogen peroxide; MitMD: mitochondrial membrane depolarization; MitROS: mitochondrial ROS; NOX: nicotinamide adenosine dinucleotide phosphate oxidase; PARP-1: poly (ADP-ribose) polymerase-1; RAC1: composed of Ras-related C3 botulinum toxin substrate; ROS: reactive oxygen species; TRP: transient receptor potential; TRPM2: transient receptor potential 2

ARTICLE HISTORY
Received 11 February 2020
Revised 21 May 2020
Accepted 24 May 2020

KEYWORDS
Apoptosis; *Clostridium botulinum* neurotoxin A; glioblastoma death; mitochondria oxidative stress; TRPM2 channel

Introduction

Glioblastoma and neuroblastoma are the most common types of primary brain tumor in adults [1,2]. Glioblastomas have most aggressive and proliferative characters within the brain tumors. Incidences of glioblastomas are two to three per hundred thousand adults per year. Neuroblastoma is the most common extracranial solid tumor of infancy. About 6% of children in cancers are suffer from neuroblastomas [3]. Hence, glioblastoma and neuroblastomas are too fatal neuronal cancer types in adults and children [4,5]. Despite significant advances in the understanding of the molecular and cellular basis of glioblastoma and neuroblastoma proliferation, etiology of glioblastomas and neuroblastomas has not been fully clarified yet.

Reactive oxygen species (ROS) are produced during the physiological and pathophysiological activities including mitochondrial function in normal neuron and brain tumors [6,7]. Excessive production of ROS induces an increase of intracellular calcium ion (Ca^{2+}) concentration in cancer cells and the calcium ion Ca^{2+} has a main role in the tumor progression, apoptosis and death [7,8]. Therefore, several subgroups of transient receptor potential (TRP) superfamily

CONTACT Mustafa Nazıroğlu mustafanaziroglu@sdu.edu.tr Department of Biophysics, Faculty of Medicine, Suleyman Demirel University, Isparta 32260, Turkey

© 2020 Informa UK Limited, trading as Taylor & Francis Group

cation channels are activated in cancer cells by the excessive ROS generation [9,10]. First discovered the oxidative-stress-dependent activated cation channels within the TRP superfamily is TRP melastatin 2 (TRPM2) and it is activated by hydrogen peroxide (H_2O_2) and ADP-ribose (ADPR) [11,12]. Involvement of TRPM2 channel activation-induced excessive Ca^{2+} entry and ROS production in several cancers has been reported in the progression of human laryngeal squamous cancer [13], DBTRG glioblastoma cells [14], and SH-SY5Y neuroblastoma cell lines [15–17]. Botulinum toxin substrate-induced excessive ROS production was recently reported in phagocytic and acute myeloid cells [18]. The oxidative induced-TRPM2 activation may play a crucial role in *Clostridium botulinum* neurotoxin A (BTX)-induced DBTRG and SH-SY5Y nerve toxicity and death.

The *Clostridium botulinum* neurotoxin with seven serotypes (A-G) are polypeptide produced by the bacterium *Clostridium botulinum*. Scientific progresses in the last decades facilitated using the polypeptides of *Clostridium botulinum* neurotoxins. A protease content of BTX inhibits the acetylcholine release at the neuromuscular junction. Type A (BTX) of the *Clostridium botulinum* neurotoxins is extensively being used as therapeutics against pain, epilepsy, ophthalmological, and neuromuscular disorders [19,20]. It has also been used to remove wrinkles and frown line from our body. In addition, recent data indicate its anticancer actions against tumor cell proliferation, including human neuroblastoma and glioblastoma tumor cells through stimulation of ROS production, apoptosis, caspase-3 and -9 activities [21–23]. However, molecular mechanisms of BTX on anticancer action in human neuroblastoma and glioblastoma tumor cells has not been clarified yet.

In this study, we examined whether the blockade of the TRPM2 channel effectively prevented BTX-induced DBTRG glioblastoma and SH-SY5Y neuroblastoma cell proliferation, oxidative toxicity and neuronal death, mediated by mitochondria-dependent ROS and TRPM2 channel signaling pathways.

Materials and methods

Cell culture

SH-SY5Y and DBTRG cell lines were purchased from Şap Institue (Ankara, Turkey). They were cultured, as previously described [24,25]. In brief, the SH-SY5Y cells were maintained in Dulbecco's modified Eagle's medium (DMEM, low glucose as 1 g/l) and Ham's F12 (50:50) medium, although DTBTG cells were maintained in the 90% DMEM. Both cell culture medium was also supplemented with 10% fetal calf serum, 2 mM glutamine, 100 IU penicillin, 100 μg/ml streptomycin in 5% CO_2 plus humidified air at 37 C. The medium and chemicals were purchased from Thermo Fischer Scientific Inc. (Istanbul, Turkey). In the laser confocal microscope (LSM800, Zeiss, Ankara Turkey) analyses, the cells were seeded in 35 mm glass bottom dishes (Mattek Corporation Inc., Ashland, MA).

Study groups of SH-SY5Y cells

Natural expressions of TRPM2 without DNA transfection were recently reported in the DBTRG glioblastoma and SH-SY5Y neuroblastoma cells [14–16]. The DBTRG and SH-SY5Y cells were divided into four groups as follows:

Control group: The DBTRG and SH-SY5Y cells were kept in a cell culture medium for 24 h.
BTX group: The DBTRG and SH-SY5Y cells were incubated with 5 IU BTX (Botox-100, Allergan Drugs Inc., Istanbul, Turkey) for 24 h [26].
BTX + ACA group: After 24 h incubation of BTX, the DBTRG and SH-SY5Y cells were further incubated with 25 μM N-(p-amylcinnamoyl) anthranilic acid (ACA) for 30 min [24].
BTX + 2-APB group: After 24 h incubation of BTX, the DBTRG and SH-SY5Y cells were incubated with 100 μM 2-aminoethyl diphenylborinate (2-APB) for 30 min [24].

Stock ACA and 2-APB solutions were dissolved in the 0.1 mm DMSO before dilution in the cell culture medium plus extracellular buffer with calcium (1.2 mM). In some experiments, the cells were stimulated by H_2O_2. The H_2O_2 was diluted in the extracellular buffer with calcium (1.2 mM) as described in previous studies [9,20]. The final concentration of H_2O_2 was 1 mM.

Assay of cell viability and cell number

After removing medium by centrifugation (1500 g for 5 min), the DBTRG and SH-SY5Y cells were diluted in the Casy tone solution as described in previous studies [13,17]. Then the cells were automatically counted in an automatic cell counter (Casy Modell TT, Roche, Germany). In addition to the cell number changes, cell viability was monitored through electrical current exclusion by the cell counter. The cell number and cell viability were expressed as 10^6/ml and %, respectively.

Imaging cell death in the SH-SY5Y cells using laser confocal microscopy

Living and dead cells undergoing laser confocal microscope analysis (LSM800) were assayed using Hoechst-33342 (3 μg/ml for 30 min) and propidium iodide (PI, 5 μg/ml for 30 min) (Cell Signaling Technologies) fluorescent dyes following the manufacturer's instructions in dark incubator medium (5% CO_2 and 37 °C) according to previous descriptions [13,14,17]. Excitation, detection, and diode laser wavelengths of Hoechst-33342 were 346, 455, and 405 nm, respectively. Excitation, detection, and diode laser wavelengths of PI were 305, 617, and 561 nm, respectively. Living/dead analysis of the cells stained with PI and Hoechst was performed by using ImageJ software. The PI/Hoechst rate results were expressed as % of dead cells.

Imaging early and late apoptosis in the DBTRG cells using laser confocal microscopy

It is well known that Phosphatidylserine residue on the cell surface is an indicator of early apoptosis. Annexin V FITC (aV-FITC) staining is a valuable method for detecting apoptotic cells, because it has high affinity in the cell for binding Phosphatidylserine residues and display green fluorescence. Propidium iodide (PI) is widely used in conjunction with aV-FITC for detection of late apoptosis, because live and early apoptotic cell with an intact plasma membrane was not stained with PI. Hence, PI as indicator of late apoptosis can easily pass the decreased integrity of the plasma and nuclear membranes, and displays red fluorescence of DNA damage [27].

The effects of BTX-induced early and apoptosis were determined by the laser confocal microscope (LSM800) fitted with a 10× objective using the aV-FITC (1 μl/ml for 30 min) and PI (5 μl/ml for 30 min) stains as described in the manufacturer's guidelines (Santa Cruz Biotechnology, Istanbul, Turkey) [14]. Excitation, detection, and diode laser wavelengths of PI in the ZEN program were 305, 617, and 561 nm, although excitation, detection, and diode laser wavelengths of aV-FITC were 495, 519, and 488 nm, respectively. Fluorescence intensity as arbitrary unit/cell was used for expression of aV-FITC and PI concentrations.

Measurements of cytosolic free Ca^{2+} concentration ($[Ca^{2+}]_c$) through TRPM2 activation in the DBTRG and SH-SY5Y cells

Intracellular changes in the free Ca^{2+} fluorescence concentration ($[Ca^{2+}]_c$) in the DBTRG and SH-SY5Y cells were monitored in dark conditions using 1 μM Fluo-3 fluorescent dye (Calbiochem, Darmstadt, Germany) visualized by a laser confocal microscope fitted with a Plan-Apochromat 40x oil objective. The Fluo-3 displays green fluorescence of ($[Ca^{2+}]_c$ and it is a single wavelength excitation (506 nm) and emission (528 nm) dye that is excited by a 488 nm argon laser from the laser confocal microscope (LSM 800) [14]. Detection wavelengths of Fluo-3 were kept between 450 and 700 nm. The microscope model was Axio ObserverZ1/7 (Zeiss). The level of Fluo-3 in 15 μm^2 of cytosol in each DBTRG or SH-SY5Y cell was expressed as the mean fluorescence intensity as arbitrary unit per cell.

Imaging mitochondrial membrane potential (MitMD) in the SH-SY5Y by the laser confocal microscope analyses

For imaging of MitMD, the cells were incubated with JC-1 fluorescent dye for 15 min at 37 °C in dark conditions [28]. The samples were then analyzed using the laser confocal microscope (LSM 800) fitted with a Plan-Apochromat 40 × 1.3 oil DIC (UV) VIS-IR M27 objective. JC-1 dye in the cells was excited with a diode laser at 488 nm [13,14]. Detection wavelengths of JC-1 were kept between 585 and 700 nm. Fluorescence intensity (arbitrary unit/cell) was used for expression of JC-1.

Imaging ROS generation in the mitochondria and cytosol of DBTRG and SH-SY5Y using laser confocal microscopy

Mitochondrial ROS (MitROS) generation visualized under laser confocal microscopy (LSM 800) by using MitoTracker Red CM-H2Xros fluorescent dye (Life Technologies) following the manufacturer's instructions. Cytosolic ROS production was monitored using two different fluorescent dyes: DHR123 and DCFH-DA. After exposure to the described treatments, the neurons were incubated with 100 nM MitoTracker Red CM-H2Xros for 30 min [13,14], then further incubated with 1 μM DCFH-DA and DHR123 for 30 min at 37 °C in dark conditions [28]. After washing the cells with 1 × PBS prior to imaging, MitoTracker Red CM-H2Xros was excited with a diode laser at 561 nm and its detection wavelength was kept between 570 and 700 nm (Excitation: 576 nm; Emission: 598 nm). DHR123 and DCFH-DA were excited with a diode laser at 488 nm. Detection wavelengths of DHR123 were kept between 400 and 575 nm (Excitation: 507 nm; Emission: 529). Detection wavelengths of DHR123 were kept between 410 and 570 nm (Excitation: 504 nm; Emission: 525 nm). The Plan-Apochromat 40x oil objective was used in the analyses of ROS.

Assay of caspase -3 and -9 activities

The determinations of caspase-3 and -9 activities in the DBTRG and SH-SY5Y cells were based on a method previously reported [24,25] with minor modifications. Caspase-3 (N-acetyl-Asp-Glu-Val-Asp-7-amido-4-methylcoumarin) and −9 (N-acetyl-Leu-Glu- His-Asp-7-amino-4-methylcoumarin) substrates were purchased from Bachem (Bubendorf, Switzerland) and cleavages of the substrates were measured with a microplate reader (Infinite pro200; Tecan Austria GmbH, Groedig, Austria) . The data were calculated as fluorescence units/mg protein and presented as fold-increase over the pretreatment level (experimental/control).

Statistical analysis

Statistical analyses were conducted using SPSS Statistical program (17.0, SPSS Inc. Chicago, IL) with the Mann–Whitney test. Data were represented as mean ± standard deviation (SD) and a p value < 0.05 was defined as significance.

Results

Inhibition of TRPM2 channel diminished BTX-induced neuron death in the DBTRG and SH-SY5Y cells

In this study, we investigated the involvement of TRPM2 channel in the cell viability *via* an electronic cell counter and cell death using PI and Hoechst fluorescent dyes. Bright field (BF) black/white images and mean values of cell number and cell viability in the DBTRG cells were indicated in Figure 1(a–c), respectively. The PI and Hoechst mean values of cell death (PI/Hoechst rate) of SH-SY5Y cells were shown in Figure 2(a,b), respectively. The cell number and cell viability levels were decreased in the BTX group of DBTRG cells by the BTX treatment, although the cell death rate was

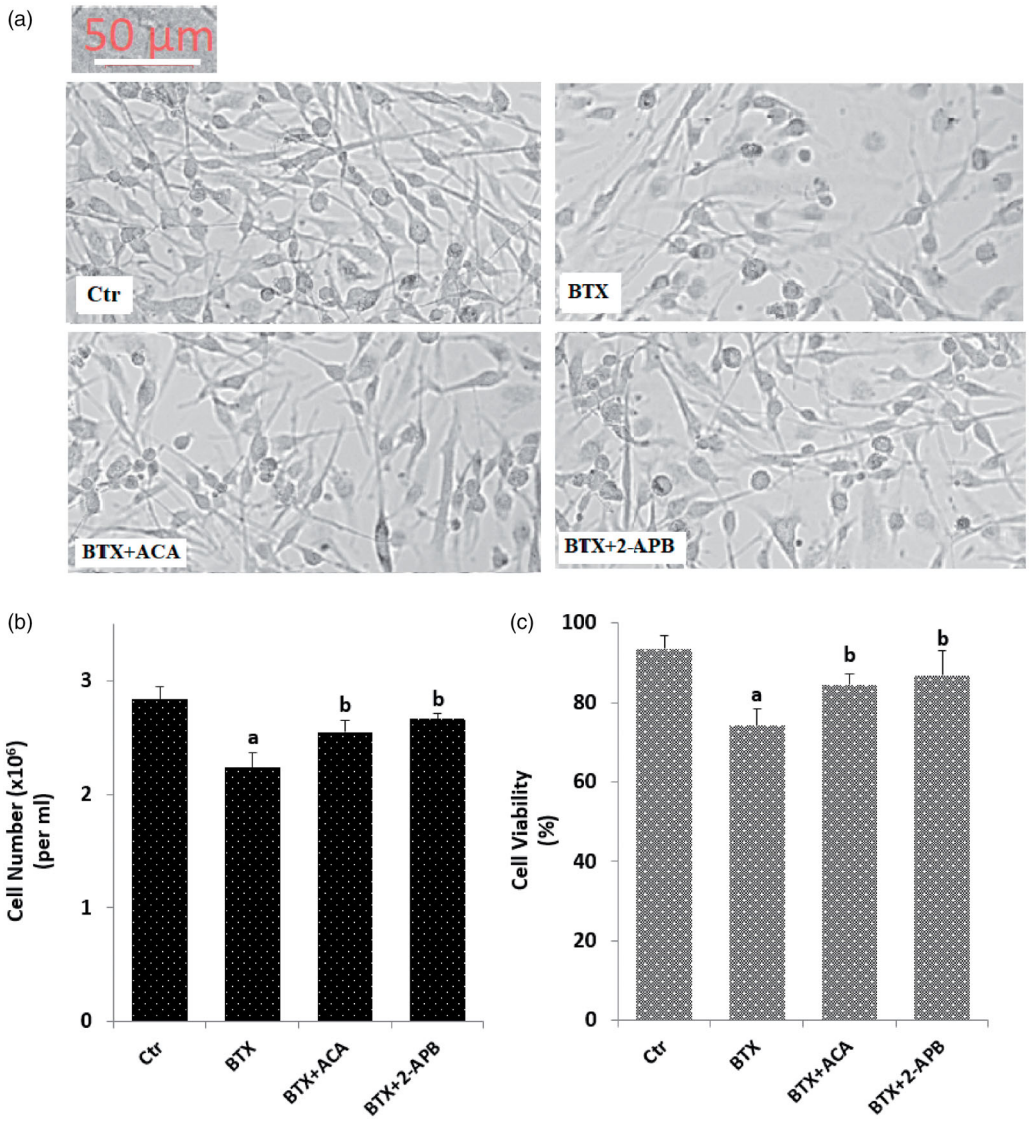


Figure 1. BTX-induced increases of DBTG cell number and viability were diminished by ACA and 2-APB treatments. (a) Representative confocal image showing bride field (BF) black/white in the four groups of the DBTRG cells. Scale bar is 50 µm. The neurons were analyzed in the laser confocal microscope (LSM 800) fitted with a 10× objective. (b, c) Summary of the mean cell number and cell viability values under control and treatment conditions. The cell values of the four groups were measured in an automatic cell counter by using Casytone counting solution. $^{a}p < 0.001$ indicate significant difference from control (Ctr) group. $^{b}p < 0.001$ indicate significant difference from BTX groups.

increased in the SH-SY5Y cells by the treatment ($p < 0.001$). However, the cell number and cell viability level in the DBTRG cell was increased by the ACA and 2-APB treatments, whereas the cell death rate in the SH-SY5Y cell was decreased by the treatments ($p < 0.001$). We found an increase in the DBTRG and SH-SY5Y cell death, but a decrease in cell proliferation following the BTX treatment. However, the BTX-induced increase of death and decrease of cell proliferation in the DBTG and SH-SY5Y was completely inhibited by the TRPM2 channel blockers (ACA and 2-APB), indicating that BTX-induced TRPM2 activation is critical in the neuroblastoma and glioblastoma cell deaths and proliferations.

BTX induced excessive Ca^{2+} influx through TRPM2 channel activation in the BTRG and SH-SY5Y cells

It is well known that cell death and tumor cell proliferation were induced ROS-induced excessive Ca^{2+} influx. After observing an increase in the cell death, but decrease in the cell proliferation by the BTX treatment, we suspected ROS-induced increase in the cytosolic Ca^{2+} concentration through the TRPM2 channel activity. The fluorescence intensity of $[Ca^{2+}]_c$ in the DBTRG and SH-SY5Y cells is shown in Figures 3 and 4, respectively. The fluorescence intensity in the basal level was increased in the BTX groups compared to control group of DBTRG (Figure 3(a)) and SH-SY5Y cells (Figure 4(a)) ($p < 0.001$). In addition, the fluorescence intensities were further increased by the H_2O_2 treatments and they were significantly higher in the BTX + H_2O_2 groups than in the BTX groups of DBTRG (Figure 3(b)) and SH-SY5Y cells (Figure 4(b)) ($p < 0.001$). However, the H_2O_2-induced fluorescence intensities were reduced in the TRPM2 channel blocker (ACA and 2-APB) groups and they were lower in the BTX + ACA + H_2O_2 and BTX + 2-APB + H_2O_2 groups than in the BTX + H_2O_2 groups of DBTRG (Figure 3(d)) and SH-SY5Y cells (Figure 4(d)) ($p < 0.001$).

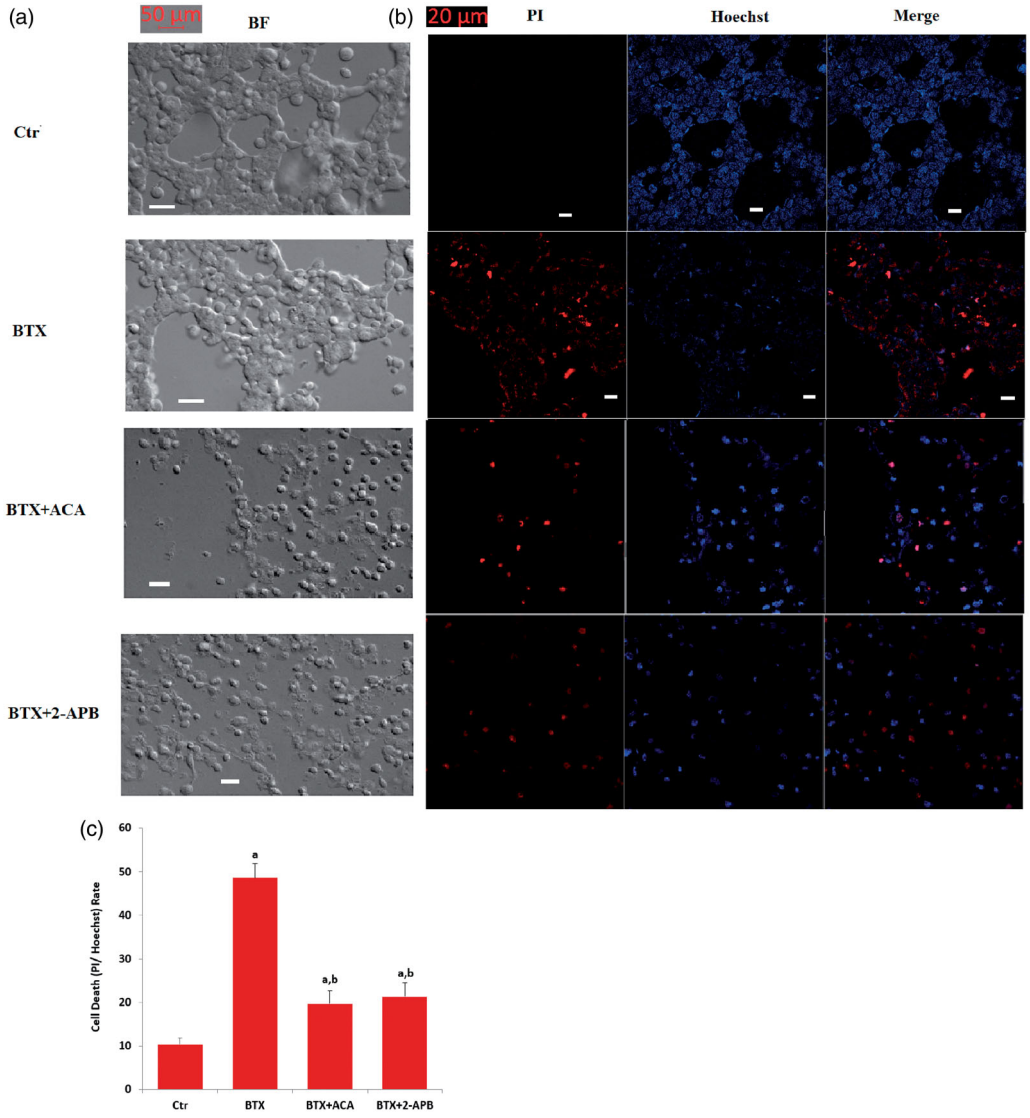


Figure 2. BTX-induced increases of SH-SY5Y neuronal cell death were diminished by ACA and 2-APB treatments. ($N = 6$ and mean ± SD). (a, b) Representative confocal images showing bright field (BF) and dead (propidium iodide-PI)/living (Hoechst) rate in the five groups. **c)** Summary of the mean fluorescence intensities of PI/Hoechst rate. Scale bar for BF and PI/Hoechst were 50 and 20 µm, respectively. Live and death neurons were analyzed in the laser confocal microscope (LSM 800) fitted with a 20× oil objective. The living and dead cells were counted using Image j program. The results were expressed as percentage changes. [a] $p < 0.001$ indicates significant difference from control (Ctr) and Se groups. [b] $p < 0.001$ indicates significant difference from BTX group.

BTX-induced increases of mitochondrial membrane depolarization (MitMD), mitochondrial and cytosolic ROS production in DBTRG and SH-SY5Y were diminished by the TRPM2 channel blockers

Accumulating evidence indicates that excessive ROS production-induced Ca^{2+} signaling triggers an increase of MitMD [29,30]. In turn, the increased MitMD in the inner membranes of mitochondria stimulates an increase of mitochondrial ROS production. Stimulation of the TRPM2 channel in the DBTRG and SH-SY5Y cells were activated by ROS [14–17]. BTX had anticancerogenic actions *via* stimulation of MitMD and ROS production in prostate tumor cell [21], breast cancer cell [22], and SH-SY5Y neuroblastoma cells [23]. After observing an increase of $[Ca^{2+}]_c$ *via* TRPM2 activation, we investigated changes of MitMD, MitROS, and cytosolic ROS productions *via* TRPM2 activation in the glioblastoma and neuroblastoma tumor cells.

Fluorescence intensities and mean values of MitMD (JC-1) and cytosolic ROS (Rh123) production in the DBTRG (Figure 5(a,b)) and SH-SY5Y (Figure 6(a,b)) cells are shown in the Figures 5 and 6, respectively. Fluorescence intensities and mean values of MitROS and cytosolic ROS (DCF-ROS) production in the SH-SY5Y cells are shown in Figure 7(a,b). The fluorescence intensities of MitMD, cytosolic ROS (Rh123 and DCF-ROS), and MitROS levels in the DBTRG and SH-SY5Y cells were higher in the BTX group than in the control group ($p < 0.001$). However, they were diminished in the BTX + ACA and BTX + 2-APB groups by the ACA and 2-APB ($p < 0.001$). Inhibitions of TRPM2 channel through ACA and 2-APB treatments have been shown to be effective in inhibiting H_2O_2-induced TRPM2-mediated neuron death and ROS production [24,25]. Involvement of TRPM2 channel in the glioblastoma and neuroblastoma mitochondrial oxidative toxicities was further confirmed by the inhibitory effect of ACA and 2-APB

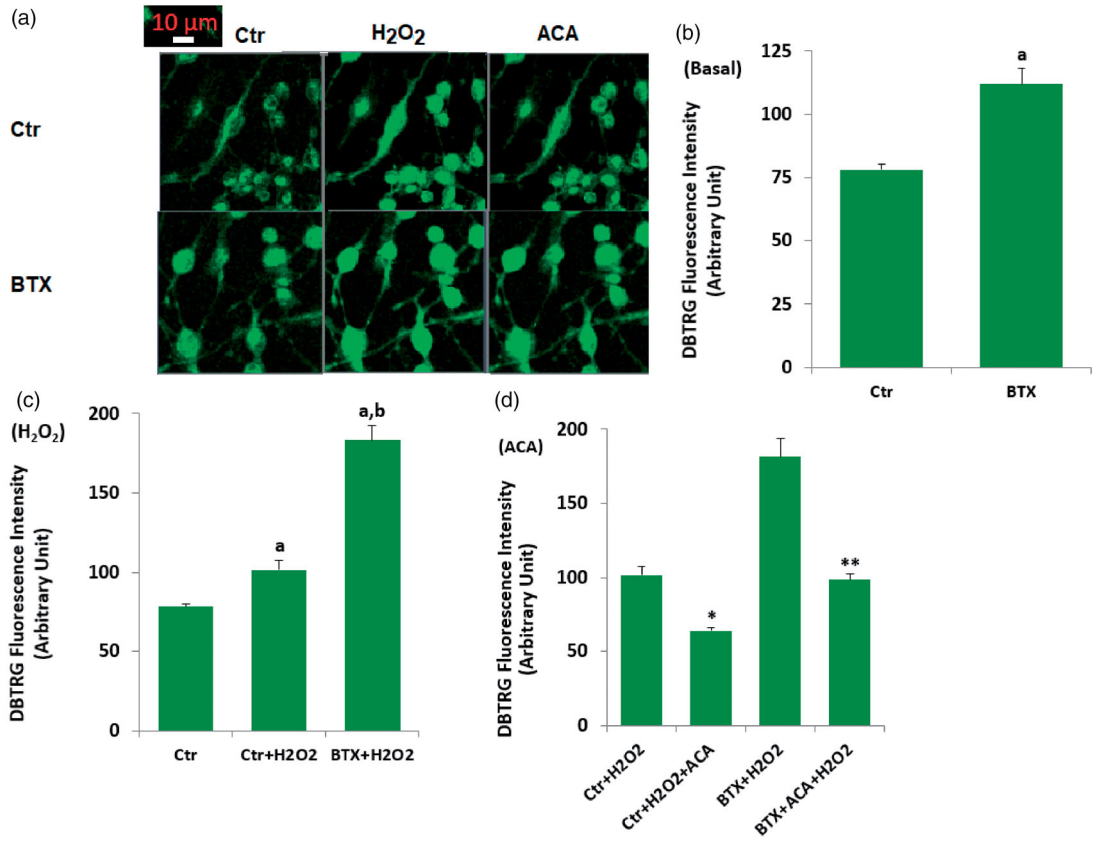


Figure 3. BTX increased $[Ca^{2+}]_c$ fluorescence intensity *via* stimulation of TRPM2 channel in the DBTRG cells. ($N = 6$ and mean ± SD). (a) Representative confocal image showing Fluo-3 in the two groups of DBTRG cells. Scale bar is 10 µm. (b–d) Summary of the mean fluorescence intensity of Fluo-3 under basal (without H_2O_2 stimulation), H_2O_2 (with H_2O_2 stimulation) and ACA treatment (with H_2O_2 stimulation and ACA incubation) condition. The neurons were analyzed at 488 nm using the laser confocal microscope fitted with a 10× objective. The fluorescence intensity of Fluo-3 was indicated as the arbitrary unit of per cell. $^{a}p < 0.001$ indicate significant difference from control (Ctr) group. $^{b}p < 0.001$ and $^{*}p < 0.001$ indicate significant difference from Ctr + H_2O_2 group. $^{**}p < 0.001$ indicate significant difference from BTX + H_2O_2 group.

on the MitMD, MitROS, and cytosolic ROS concentrations in the DBTRG and SH-SY5Y cells.

Stimulation of TRPM2 channel through BTX-induced oxidative stress increased apoptosis through inhibition of caspase-3 and -9 activities in the DBTRG and SH-SY5Y cells

In addition to the excessive ROS production, increase of MitMD results in apoptosis through activation of caspase-3 and 9 activities. However, modulation of TRPM2 results in the decrease of apoptosis through inhibition of caspase-3 and -9 activities in the DBTRG and SH-SY5Y cells. However, the involvement of the apoptosis level and caspase activities *via* activation of TRPM2 has not been clarified yet. In this study, we investigated the involvement of TRPM2 channel in the caspase activities, early (aV-FITC) and late (PI) apoptosis levels. The images and mean values of aV-FITC and PI stains were shown in the in the DBTRG cells were indicated in Figure 8(a,b). The caspase-3 and -9 activities in the DBTRG (Figure 9(a)) and SH-SY5Y (Figure 9(b)) are shown in Figure 9. The caspase activities, aV-FITC and PI levels were upregulated in the BTX group in the DBTRG and SH-SY5Y cells by the BTX treatment, although they were diminished in the cells by the ACA and 2-APB treatments ($p < 0.001$). We found an increase in the DBTRG and SH-SY5Y cell apoptosis through caspase-3 and -9 activations following the BTX treatment. However, the BTX-induced increase of early and late apoptosis in the DBTG and caspase-3 and -9 activities in the DBTRG and SH-SY5Y cells were completely inhibited by the TRPM2 channel blocker (ACA and 2-APB) treatments, indicating involvement of BTX-induced TRPM2 activation in the neuroblastoma and glioblastoma cell apoptosis.

Discussion

Glioblastoma and neuroblastoma are the most common and fetal types of brain tumor in adult and children, respectively. The progressions and treatments of glioblastoma and neuroblastoma have not fully discovered yet. However, results of recent studies indicate that BTX can inhibit of glioblastoma and neuroblastoma tumor invasion *via* stimulation of apoptosis and ROS [21–23]. The apoptotic and oxidant actions of overload Ca^{2+} influx in DBTRG and SH-SY5Y cells were recently reported [14–17], although the apoptotic and oxidant effect and molecular mechanism of BTX in the cells have not previously been investigated. In this study, we examined the potential protective effect of apoptotic and oxidant effect against using DBTRG and SH-SY5Y cell line models. We demonstrated that BTX exerts a major protective

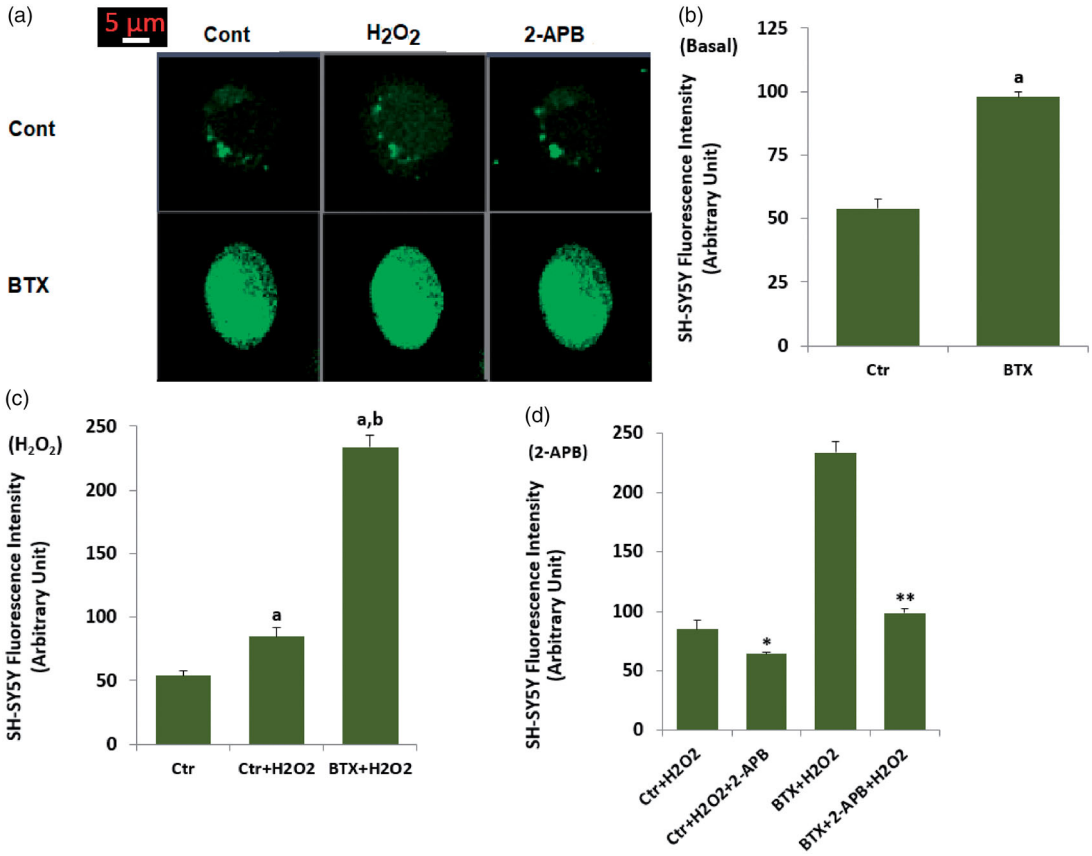


Figure 4. BTX increased $[Ca^{2+}]_c$ fluorescence intensity *via* stimulation of TRPM2 channel in the SH-SY5Y cells. ($N = 6$ and mean ± SD). (a) Representative confocal image showing Fluo-3 in the two groups of SH-SY5Y cells. Scale bar was 5 µm. (b–d) Summary of the mean fluorescence intensity of Fluo-3 under basal (without H_2O_2 stimulation), H_2O_2 (with H_2O_2 stimulation) and 2-APB treatment (with H_2O_2 stimulation and 2-APB incubation) condition. The neurons were analyzed at 488 nm using the laser confocal microscope fitted with a 40× oil objective. The fluorescence intensity of Fluo-3 was indicated as the arbitrary unit of per cell. $^{a}p < 0.001$ indicate significant difference from control (Ctr) group. $^{b}p < 0.001$ and $^{*}p < 0.001$ indicate significant difference from Ctr + H_2O_2 group. $^{**}p < 0.001$ indicate significant difference from BTX + H_2O_2 group.

effect on the DBTRG and SH-SY5Y proliferation *via* stimulation of apoptosis and cell death and that the underlying molecular mechanisms may be upregulation of mitochondria-related oxidative stress pathways and TRPM2 activation.

It is well known that cancer cell proliferation is arranged by the $[Ca^{2+}]_c$. Excessive ROS production stimulates apoptosis and cell death in the tumor cells including DBTRG and SH-SY5Y cells. Hence, chemotherapeutic agents such as cisplatin and docetaxel kill the cancer cells through excessive production of ROS and Ca^{2+} influx [14,15,25,31]. Oxidant and apoptotic roles of BTX were recently reported in cancer and normal cells [21–23]. On the subject, it was reported that nicotinamide adenosine dinucleotide phosphate oxidase (NOX) is composed of Ras-related C3 botulinum toxin substrate 1 (RAC1) and NOX-induced increases of lipid peroxidation and oxidative stress levels *via* RAC1 were increased in rats by menopause-associated learning and memory impairments [32]. In addition, an increase of RAC1-induced mitochondrial ROS in endothelial cells was reported by high glucose [33]. Hence, BTX and its toxin substrate (RAC1) induces excessive ROS production. TRPM2 channel is activated in several cells including DBTRG and SH-SY5Y by [14,15,25,31]. Excessive Ca^{2+} influx *via* activation of TRPM2 channel induces excessive ROS production in cancer cells [9,10]. Till today, there has been no previous report of an interaction between the BTX and TRPM2 channel-induced Ca^{2+} influx in cells and animals. In the current study, BTX-induced increases of $[Ca^{2+}]_c$ in the DBTRG and SH-SY5Y cells were decreased by treatment with the TRPM2 channel blocker (ACA and 2-APB) treatments.

Accumulating evidence indicate that the inhibition of tumor cell proliferation was inhibited by excessive ROS production. In the case of BTX-caused Ca^{2+} signaling molecular pathways, there are two possible results. These signals consist in (i) an increase of MitMD and (ii) the accumulation of ROS [29,30]. Both these processes eventually occur as a result Ca^{2+} influx *via* TRPM2 channel activation [24,28], in turn resulting in the functional and physical breakdown of mitochondria followed by cell death [21,22,33,34]. In experimental animals, the oxidant effects of RAC1 involves down-regulation of the antioxidants, although up-regulation of mitochondrial ROS [33,34]. Moreover, BTX has been shown for downregulate different gene relevant to proliferation in cancer cell lines [35–38]. In this study, we observed for the first time that treatment of BTX elevated apoptosis, cell death, mitochondrial and cytosolic ROS, and the up-regulation of TRPM2 channel activity in the DBTG and SH-SY5Y cells. However, the BTX-induced decrease of cell number and

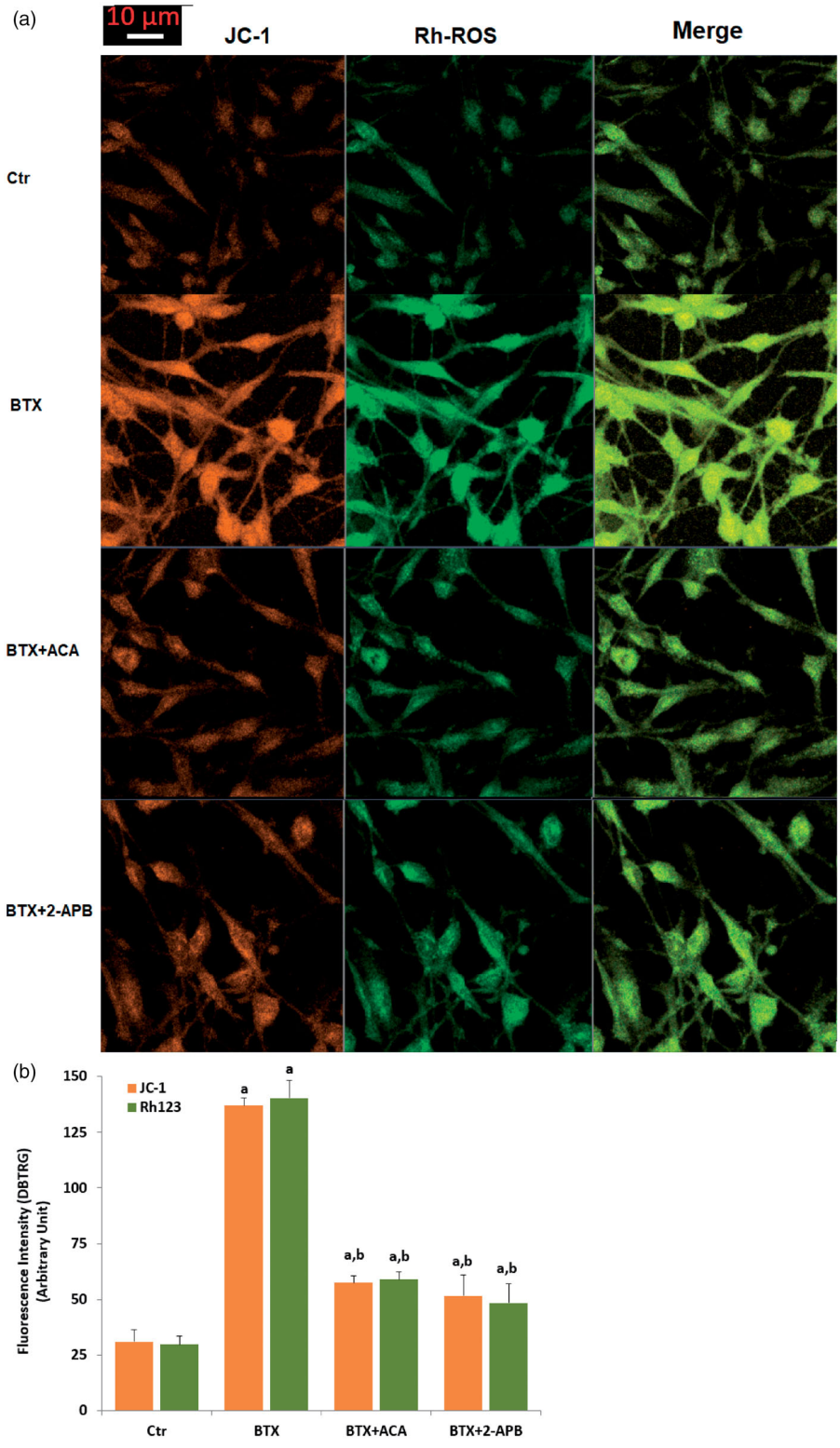


Figure 5. BTX-induced increases of mitochondrial membrane depolarization (MitMD) and cytosolic ROS (Rh123) production in the DBTRG cells were reversed by the ACA and 2-APB treatments. ($N = 6$ and mean ± standard deviation). (a) Representative confocal image showing JC-1 and Rh123 in the control, BTX, BTX + ACA, and BTX + 2-APB groups. The scale bar was 10 µm. (b) Summaries of the mean fluorescence intensities of JC-1 and Rh123. The DBTRG cells were analyzed at 488 nm using a laser confocal microscope fitted with a 10× objective. The fluorescence intensities of JC-1 and Rh123 were measured by then ZEN program. [a]$p < 0.001$ indicate significant difference from control (Ctr) group. [b]$p < 0.001$ indicate significant difference from BTX.

proliferation was increased by the ACA and 2-APB treatment. In addition, ACA and 2-APB treatments evidently modulated the increase in apoptosis, cell death, mitochondrial, and cytosolic ROS productions. Hence, stimulation of the TRPM2 channel resulted in oxidant and apoptotic actions in the BTX-induced oxidative damage and cell death in the DBTRG and SH-SY5Y cells. Similarly, BTX inhibited the growth of LNCaP human prostate cancer cells and T47D breast cancer

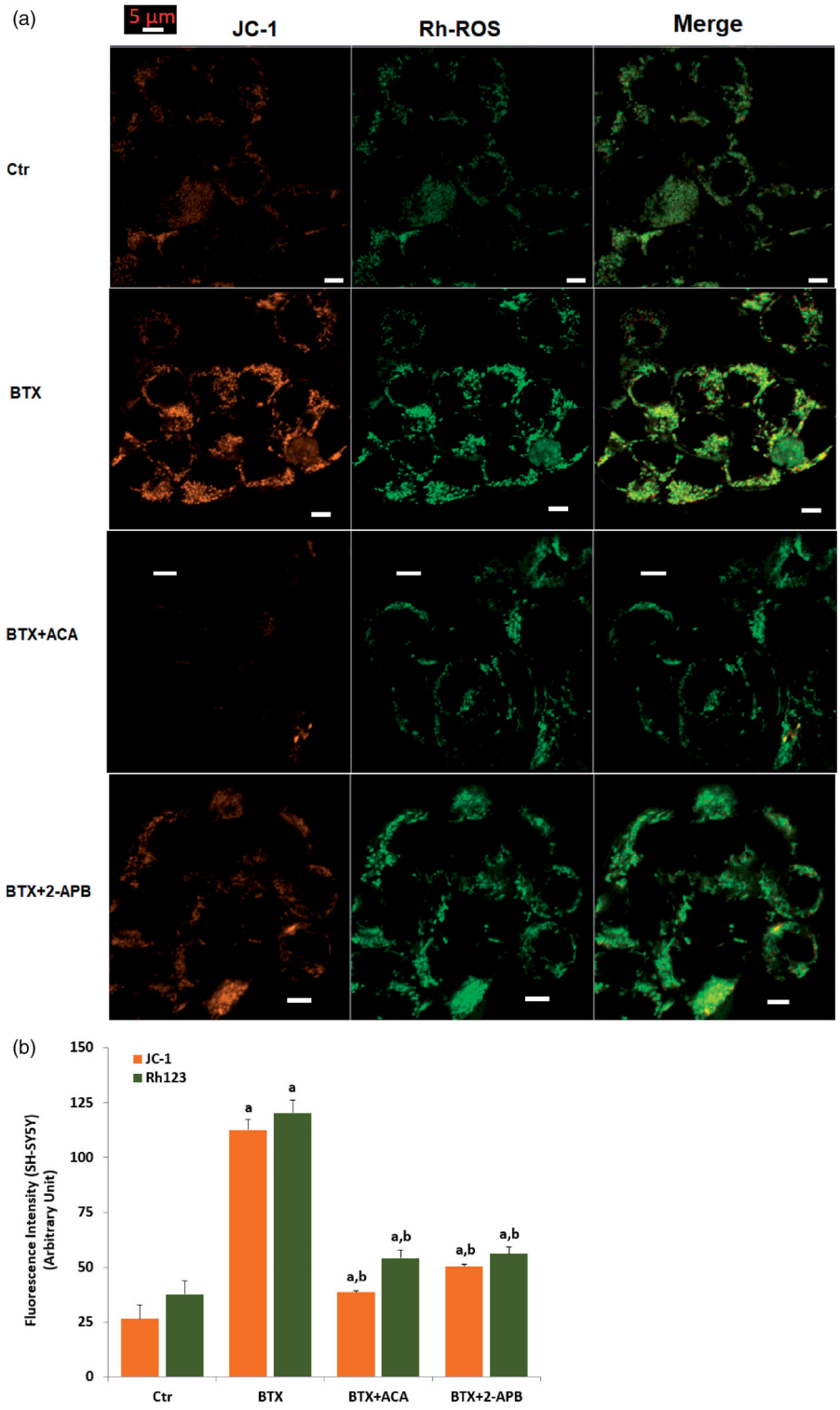


Figure 6. BTX-induced increases of mitochondrial membrane depolarization (MitMD) and cytosolic ROS (Rh123) production in the SH-SY5Y cells were reversed by the ACA and 2-APB treatments. ($N = 6$ and mean ± standard deviation). **a)** Representative confocal image showing JC-1 and Rh123 in the control, BTX, BTX + ACA and BTX + 2-APB groups. The scale bar was 5 µm. (b) Summaries of the mean fluorescence intensities of JC-1 and Rh123. The SH-SY5Y cells were analyzed at 488 nm using the laser confocal microscope fitted with a 40× oil objective. . $^{a}p < 0.001$ indicate significant difference from control (Ctr) and Se groups. $^{b}p < 0.001$ indicate significant difference from BTX.

cell line *in vitro* and *in vivo* and it induced apoptosis in a dose-dependent manner [21,22,39].

Caspase-3 and -9 are synthetized as inactivated pro-caspases and then they were rapidly activated by several factors including excessive ROS production [24]. Activation of initiator caspases including caspase-3 trigger cascade for inducing apoptosis [29,30]. Previously, it was reported that BTX induces caspase independently neuronal apoptosis in normal cells [37,40]. However, BTX potentiated chemotherapeutic agent treatment in several cancer types. Hence, the

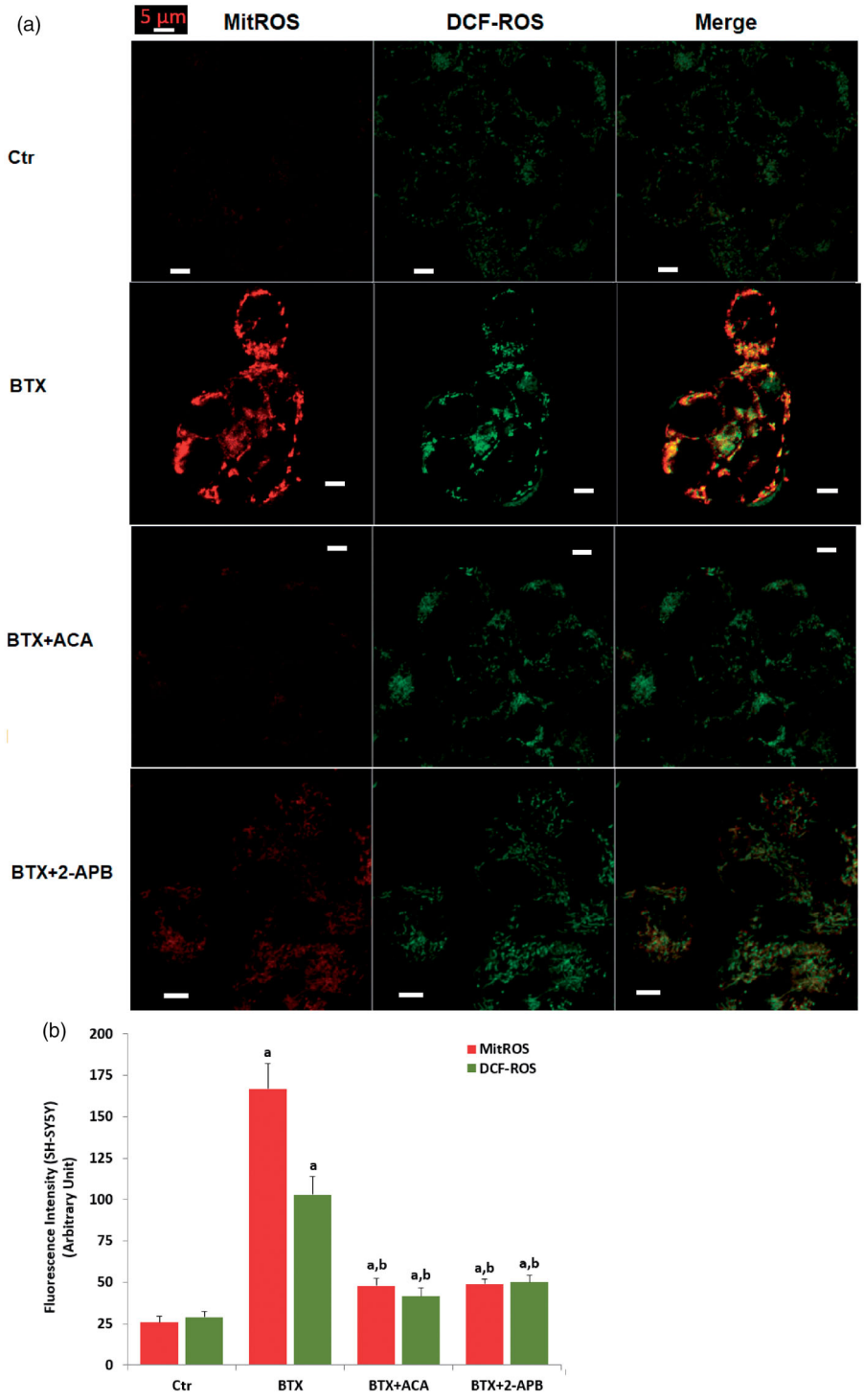


Figure 7. BTX-induced increases of mitochondrial (MitROS) and cytosolic ROS (DCFH-DA) production in the SH-SY5Y cells were decreased by inhibition of TRPM2 channel. ($N = 6$ and mean ± standard deviation). (a) Representative confocal image showing MitROS assay and DCFH-DA (DCF-ROS) assay in the four groups. Scale bar was 5 µm. b) Summaries of the mean fluorescence intensities of MitROS and DCF, respectively. MitROS and DCFH-DA in the neuronal cells were analyzed at 561 and 488 nm laser stimulation, respectively. In the both analyses, the laser confocal microscope was fitted with a 40× oil objective. The fluorescence intensities of MitROS and DCF-ROS were indicated as the arbitrary unit per cell. [a] $p < 0.001$ indicate significant difference from control (Ctr) group. [b] $p < 0.001$ indicate significant difference from BTX.

increase of caspase activities *via* an increase of mitochondria ROS production in the tumor cells after BTX treatment was reported [21–23,37]. Similarly, we observed an increase of caspase-3 and -9 activities *via* mitochondria and cytosolic ROS in the DBTRG and SH-SY5Y cells after BTX treatment and they may be due to an upregulation in oxygenation and perfusion in the tumor cells [41]. There is no report interaction between TRPM2 channel activity and BTX treatment in cells. However, a decrease of caspase-3 and -9 activities *via* inhibition of TRPM2 channel in DBTRG and SH-SH5Y cells after ACA and 2-APB treatments were recently reported [14–17]. In the current study, we observed similar caspase-3

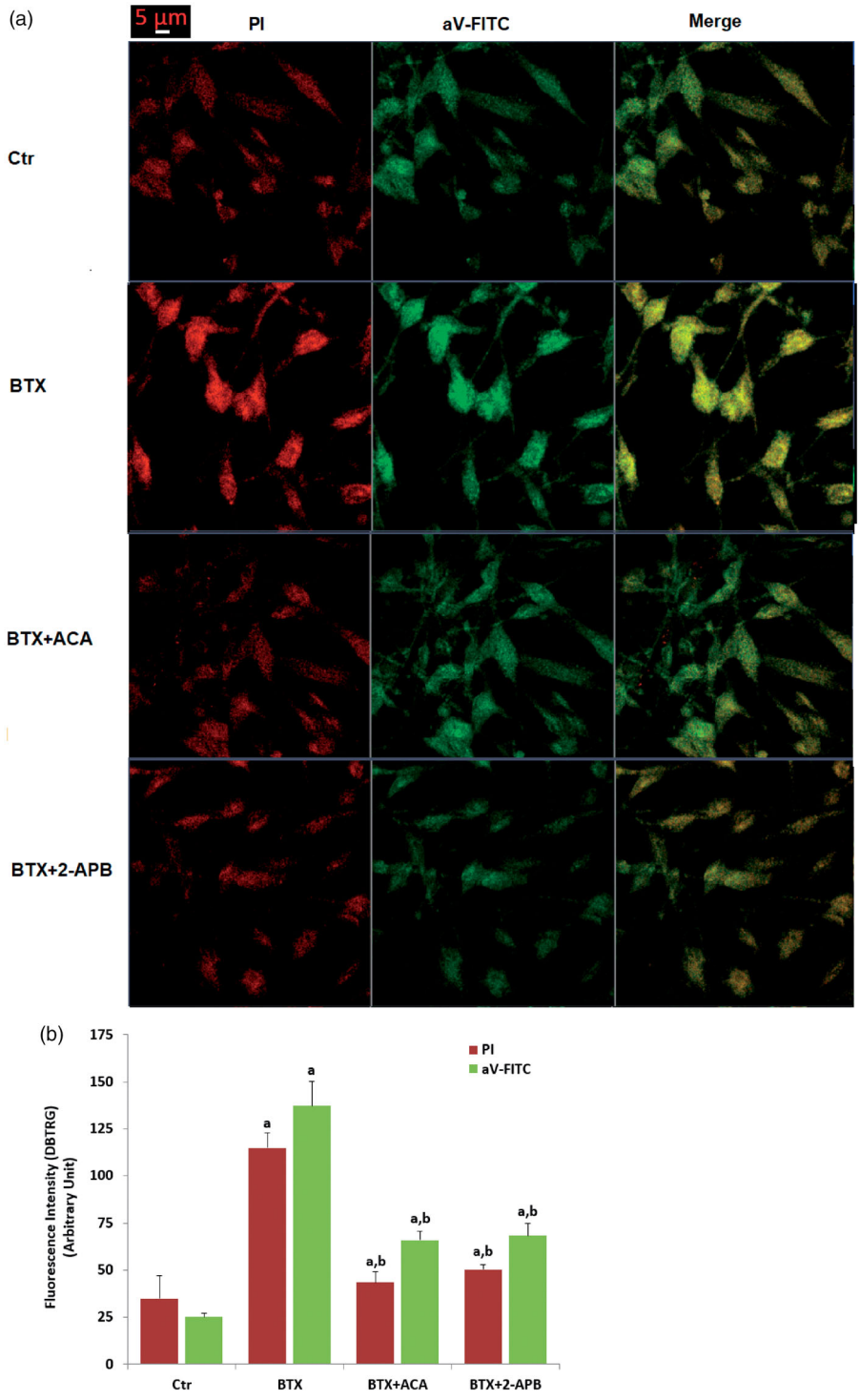


Figure 8. BTX-induced increases of apoptosis in the DBTRG cells were diminished by inhibition of TRPM2 channel. ($N = 6$ and mean ± SD). (a) Representative confocal image showing late apoptosis (propidium iodide, PI) and early apoptosis (Annexin V-FITC, aV-FITC assays in the four groups. Scale bar was 5 µm. (b) Summaries of the mean fluorescence intensities of PI and aV-FITC. In the both analyses, the laser confocal microscope was fitted with a 10× objective. $^{a}p < 0.001$ indicate significant difference from control (Ctr) group. $^{b}p < 0.001$ indicate significant difference from BTX.

and -9 results and they were markedly diminished in the DBTRG and SH-SY5Y cells by the modulation of TRPM2 channel blocker (ACA and 2-APB).

In summary, our data provide new insight into the potential anticancerogenic, apoptotic, and oxidant mechanisms of BTX-induced BTRG glioblastoma and SH-SY5Y neuroblastoma oxidative injury and death. TRPM2 channel blockers (ACA and 2-APB) treatments modulated BTX-induced mitochondrial membrane depolarization, neuronal death, and mitochondrial and cytosolic ROS levels in the BTRG and SH-SY5Y cells. In addition, ACA and 2-APB treatments diminished H_2O_2-induced TRPM2 currents and cytosolic $[Ca^{2+}]_c$ in the DBTRG and SH-SY5Y cells, suggesting a suppression of Ca^{2+} influx and cell death. Treatment with BTX may be considered

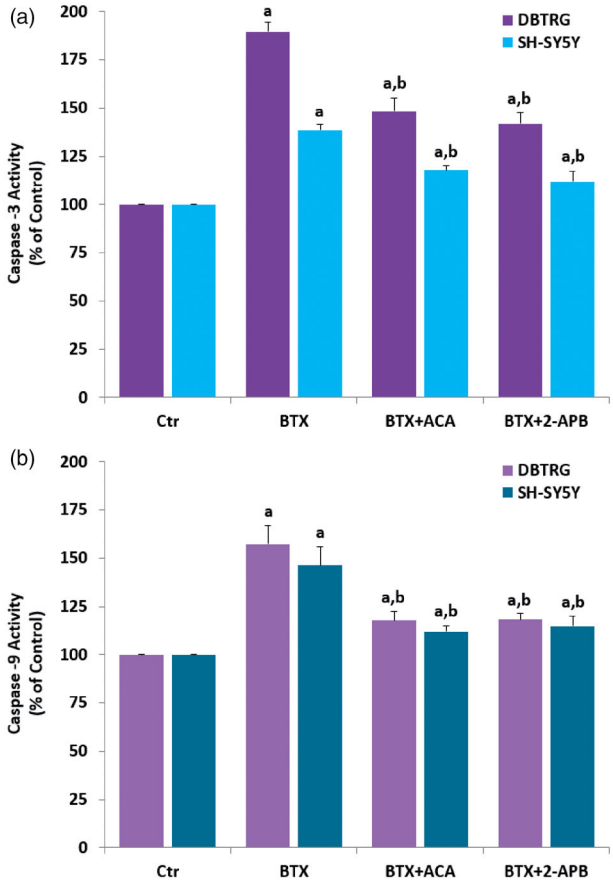


Figure 9. BTX-induced increases of caspase-3 and -9 activities in the DBTRG and SH-SY5Y cells were diminished by Se and 2-APB treatments. ($N = 6$ and mean ± standard deviation). Caspase-3 and -9 activities were analyzed in the microplate reader by using caspase substrates. The results were expressed as % of control. [a] $p < 0.001$ indicates significant difference from control (Ctr) group. [b] $p < 0.001$ indicates significant difference from BTX group.

as an anticancerogenic strategy in the glioblastoma and neuroblastoma of cancer patients.

Author contributions

The cell culture, plate reader, laser confocal microscope and cell viability analyses in the current study were performed in 3rd International Brain Research School, 25 June-1 July October 2018, Isparta, Turkey by O.A., A.Ö, M.G and M.N (http://2018.brs.org.tr/). M.N. and O.A formulated the present hypothesis. M.N. wrote the report. A.Ö. and M.G. were responsible for preparation of cell culture. O.A. was also responsible for the plate reader caspase analyses. M.N. was responsible for analyzing the laser confocal microscope. A.Ö. and M.G. made critical revisions to the manuscript.

Disclosure statement

No potential conflict of interest was reported by the author(s).

Funding

The study was supported by BSN Health, Analyses, Innovation, Consultancy, Organization, Agriculture, Industry and Trade Limited Company, Göller Bölgesi Teknokenti, Isparta, Turkey (Project No: 2018-21).

ORCID

Mustafa Nazıroğlu http://orcid.org/0000-0003-0887-6974

References

[1] Ji X, Wang H, Zhu J, et al. Correlation of Nrf2 and HIF-1α in glioblastoma and their relationships to clinicopathologic features and survival. Neurol Res. 2013;35(10):1044–1050.
[2] Bhatti P, Stewart PA, Hutchinson A, et al. Lead exposure, polymorphisms in genes related to oxidative stress, and risk of adult brain tumors. Cancer Epidemiol Biomarkers Prev. 2009;18(6):1841–1848.
[3] Paquette K, Coltin H, Boivin A, et al. Cancer risk in children and young adults born preterm: A systematic review and meta-analysis. PLoS One. 2019;14(1):e0210366.
[4] Incekara F, Koene S, Vincent A, et al. Association between supratotal glioblastoma resection and patient survival: a systematic review and meta-analysis. World Neurosurg. 2019;127:617–624.
[5] Eyüpoglu IY, Savaskan NE. Epigenetics in brain tumors: HDACs take center stage. Curr Neuropharmacol. 2016;14(1):48–54.
[6] Nazıroğlu M. New molecular mechanisms on the activation of TRPM2 channels by oxidative stress and ADP-ribose. Neurochem Res. 2007;32(11):1990–2001.
[7] Nazıroğlu M, Tokat S, Demirci S. Role of melatonin on electromagnetic radiation-induced oxidative stress and Ca2+ signaling molecular pathways in breast cancer. J Recept Signal Transduct Res. 2012;32(6):290–297.
[8] Ishii M, Oyama A, Hagiwara T, et al. Facilitation of H2O2-induced A172 human glioblastoma cell death by insertion of oxidative stress-sensitive TRPM2 channels. Anticancer Res. 2007;27(6B):3987–3992.
[9] Hantute-Ghesquier A, Haustrate A, Prevarskaya N, et al. TRPM family channels in cancer. Pharmaceuticals (Basel). 2018;11(2):58.
[10] Chen SJ, Zhang W, Tong Q, et al. Role of TRPM2 in cell proliferation and susceptibility to oxidative stress. Am J Physiol, Cell Physiol. 2013;304(6):C548–560.
[11] Hara Y, Wakamori M, Ishii M, et al. LTRPC2 Ca2+-permeable channel activated by changes in redox status confers susceptibility to cell death. Mol Cell. 2002;9(1):163–173.
[12] Nazıroğlu M, Lückhoff A. A calcium influx pathway regulated separately by oxidative stress and ADP-Ribose in TRPM2 channels: single channel events. Neurochem Res. 2008;33(7):1256–1262.
[13] Gökçe Kütük S, Gökçe G, Kütük M, et al. Curcumin enhances cisplatin-induced human laryngeal squamous cancer cell death through activation of TRPM2 channel and mitochondrial oxidative stress. Sci Rep. 2019;9(1):17784.
[14] Ertilav K, Nazıroğlu M, Ataizi ZS, et al. Selenium enhances the apoptotic efficacy of docetaxel through activation of TRPM2 channel in DBTRG glioblastoma cells. Neurotox Res. 2019;35(4):797–808.
[15] Öz A, Çelik Ö. Curcumin inhibits oxidative stress-induced TRPM2 channel activation, calcium ion entry and apoptosis values in SH-SY5Y neuroblastoma cells: Involvement of transfection procedure. Mol Membr Biol. 2016;33(3-5):76–88.
[16] Li X, Jiang LH. A critical role of the transient receptor potential melastatin 2 channel in a positive feedback mechanism for reactive oxygen species-induced delayed cell death. J Cell Physiol. 2019;234(4):3647–3660.
[17] Özkaya D, Nazıroğlu M. Curcumin diminishes cisplatin-induced apoptosis and mitochondrial oxidative stress through inhibition of TRPM2 channel signaling pathway in mouse optic nerve. J Recept Signal Transduct Res. 2020;5:1–12.
[18] Sillar JR, Germon ZP, Deluliis GN, et al. The role of reactive oxygen species in acute myeloid leukaemia. Int J Mol Sci. 2019;20(23):E6003.
[19] Patil S, Willett O, Thompkins T, et al. Botulinum toxin: Pharmacology and therapeutic roles in pain states. Curr Pain Headache Rep. 2016;20(3):15.

[20] Oh HM, Chung ME. Botulinum toxin for neuropathic pain: a review of the literature. Toxins (Basel). 2015;7(8):3127–3154.
[21] Karsenty G, Rocha J, Chevalier S, et al. Botulinum toxin type A inhibits the growth of LNCaP human prostate cancer cells in vitro and in vivo. Prostate. 2009;69(11):1143–1150.
[22] Bandala C, Perez-Santos JL, Lara-Padilla E, et al. Effect of botulinum toxin A on proliferation and apoptosis in the T47D breast cancer cell line. Asian Pac J Cancer Prev. 2013;14(2):891–894.
[23] Rust A, Leese C, Binz T, et al. Botulinum neurotoxin type C protease induces apoptosis in differentiated human neuroblastoma cells. Oncotarget. 2016;7(22):33220–33228.
[24] Uğuz AC, Öz A, Nazıroğlu M. Curcumin inhibits apoptosis by regulating intracellular calcium release, reactive oxygen species and mitochondrial depolarization levels in SH-SY5Y neuronal cells. J Recept Signal Transduct Res. 2016;36(4):395–401.
[25] Oz A, Celik O, Ovey IS. Effects of different doses of curcumin on apoptosis, mitochondrial oxidative stress and calcium influx in DBTRG glioblastoma cells. J Cell Neurosci Oxid Stress. 2017;9:617–629.
[26] Yowler BC, Kensinger RD, Schengrund CL. Botulinum neurotoxin A activity is dependent upon the presence of specific gangliosides in neuroblastoma cells expressing synaptotagmin I. J Biol Chem. 2002;277(36):32815–32819.
[27] Rieger AM, Nelson KL, Konowalchuk JD, et al. Modified annexin V/propidium iodide apoptosis assay for accurate assessment of cell death. J Vis Exp. 2011;50:2597.
[28] Joshi DC, Bakowska JC. Determination of mitochondrial membrane potential and reactive oxygen species in live rat cortical neurons. J Vis Exp. 2011;51:2704.
[29] Carrasco C, Rodríguez BA, Pariente JA. Melatonin as a stabilizer of mitochondrial function: Role in diseases and aging. Turk J Biol. 2015;39:822–831.
[30] Carrasco C, Nazıroğlu M, Rodríguez AB, et al. Neuropathic pain: Delving into the oxidative origin and the possible implication of transient receptor potential channels. Front Physiol. 2018;9:95.
[31] Nur G, Nazıroğlu M, Deveci HA. Synergic prooxidant, apoptotic and TRPV1 channel activator effects of alpha-lipoic acid and cisplatin in MCF-7 breast cancer cells. J Recept Signal Transduct Res. 2017;37(6):569–577.
[32] Kan H, Hu W, Wang Y, et al. NADPH oxidase-derived production of reactive oxygen species is involved in learning and memory impairments in 16-month-old female rats. Mol Med Rep. 2015;12(3):4546–4553.
[33] Kowluru RA, Kowluru A, Veluthakal R, et al. TIAM1-RAC1 signalling axis-mediated activation of NADPH oxidase-2 initiates mitochondrial damage in the development of diabetic retinopathy. Diabetologia. 2014;57(5):1047–1056.
[34] Bandala C, Terán-Melo JL, Anaya-Ruiz M, et al. Effect of botulinum neurotoxin type A (BoNTA) on the morphology and viability of 3T3 murine fibroblasts. Int J Clin Exp Pathol. 2015;8(8):9458–9462.
[35] Thirunavukkarasusx N, Ghosal KJ, Kukreja R, et al. Microarray analysis of differentially regulated genes in human neuronal and epithelial cell lines upon exposure to type A botulinum neurotoxin. Biochem Biophys Res Commun. 2011;405(4):684–690.
[36] Gorgal T, Charrua A, Silva JF, et al. Expression of apoptosis-regulating genes in the rat prostate following botulinum toxin type A injection. BMC Urol. 2012;12:1.
[37] Nam HJ, Kang JK, Chang JS, et al. Cells transformed by PLC-gamma 1 overexpression are highly sensitive to clostridium difficile toxin A-induced apoptosis and mitotic inhibition. J Microbiol Biotechnol. 2012;22(1):50–57.
[38] Tegenge MA, Böhnel H, Gessler F, et al. Neurotransmitter vesicle release from human model neurons (NT2) is sensitive to botulinum toxin A. Cell Mol Neurobiol. 2012;32(6):1021–1029.
[39] Proietti S, Nardicchi V, Porena M, et al. Botulinum toxin type-A toxin activity on prostate cancer cell lines. Urologia. 2012;79(2):135–141.
[40] Berliocchi L, Fava E, Leist M, et al. Botulinum neurotoxin C initiates two different programs for neurite degeneration and neuronal apoptosis. J Cell Biol. 2005;168(4):607–618.
[41] Kumar R, Zhou Y, Ghosal K, et al. Anti-apoptotic activity of hemagglutinin-33 and botulinum neurotoxin and its implications to therapeutic and countermeasure issues. Biochem Biophys Res Commun. 2012;417(2):726–731.